Fiber-optic Monitoring of Spinal Cord Hemodynamics in Experimental Aortic Occlusion

Angela S. Kogler, M.S., Thomas V. Bilfinger, M.D., Robert M. Galler, M.D., Rickson C. Mesquita, Ph.D., Michael Cutrone, B.S., Steven S. Schenkel, B.E., Arjun G. Yodh, Ph.D., Thomas F. Floyd, M.D.

ABSTRACT

Background: Spinal cord ischemia occurs frequently during thoracic aneurysm repair. Current methods based on electrophysiology techniques to detect ischemia are indirect, non-specific, and temporally slow. In this article, the authors report the testing of a spinal cord blood flow and oxygenation monitor, based on diffuse correlation and optical spectroscopies, during aortic occlusion in a sheep model.

Methods: Testing was carried out in 16 Dorset sheep. Sensitivity in detecting spinal cord blood flow and oxygenation changes during aortic occlusion, pharmacologically induced hypotension and hypertension, and physiologically induced hypoxia/hypercarbia was assessed. Accuracy of the diffuse correlation spectroscopy measurements was determined *via* comparison with microsphere blood flow measurements. Precision was assessed through repeated measurements in response to pharmacologic interventions.

Results: The fiber-optic probe can be placed percutaneously and is capable of continuously measuring spinal cord blood flow and oxygenation preoperatively, intraoperatively, and postoperatively. The device is sensitive to spinal cord blood flow and oxygenation changes associated with aortic occlusion, immediately detecting a decrease in blood flow (−65 ± 32%; n = 32) and blood oxygenation (−17 ± 13%, n = 11) in 100% of trials. Comparison of spinal cord blood flow measurements by the device with microsphere measurements led to a correlation of $R^2 = 0.49$, $P < 0.01$, and the within-sheep coefficient of variation was 9.69%. Finally, diffuse correlation spectroscopy is temporally more sensitive to ischemic interventions than motor-evoked potentials.

Conclusion: The first-generation spinal fiber-optic monitoring device offers a novel and potentially important step forward in the monitoring of spinal cord ischemia. **(ANESTHESIOLOGY 2015; 123:00-00)**

THE frequency of spinal cord ischemia as a complication after descending thoracic and thoracoabdominal aortic aneurysm repair remains intolerably high,[1,2] in spite of options for stenting,[3] staged repair,[4] distal perfusion,[5] collateral vessel reimplantation,[6] and cerebrospinal fluid drainage.[7] Secondary spinal cord injuries can also occur as a complication of spinal surgeries for spinal cord tumor resection[8] and correction of spinal cord deformities such as scoliosis.[9] Thus, the development of tools for *in situ* assessment of spinal cord ischemia is desirable.

Presently, evoked potential monitoring during vascular and spinal surgery is the standard of care.[10,11] The published range for subjects with electrophysiological changes that developed paraparesis, paraplegia, or quadriplegia varies from 16 to 40%.[12] False-negative results can occur because the monitoring is pathway specific and any injury not involving that pathway will not be detected by evoked potentials.[13] Somatosensory and motor-evoked potentials (MEPs) do not directly monitor spinal cord hemodynamics; rather, they detect the result

What We Already Know about This Topic

- Spinal cord ischemia may occur during thoracic aortic aneurysm repair
- Evoked potential monitoring offers limited sensitivity and specificity in defining ischemia
- A fiber-optic probe using near-infrared spectroscopy (diffuse correlation and optical spectroscopy) can detect real-time spinal cord blood flow and oxygenation changes in sheep subjected to aortic cross-clamp

What This Article Tells Us That Is New

- The fiber-optic probe can be placed percutaneously into the epidural space of anesthetized sheep
- Changes in blood flow detected by the probe correlated with microsphere-detected changes in spinal cord blood flow during occlusion and deocclusion of the thoracic aorta
- Changes in spinal cord blood flow detected by the fiber-optic probe were markedly more rapid in onset than functional changes detected by motor-evoked responses

Supplemental Digital Content is available for this article. Direct URL citations appear in the printed text and are available in both the HTML and PDF versions of this article. Links to the digital files are provided in the HTML text of this article on the Journal's Web site (www.anesthesiology.org).

Submitted for publication December 26, 2014. Accepted for publication August 5, 2015. From the Departments of Anesthesiology (A.S.K., M.C., T.F.F.), Surgery (T.V.B.), and Neurological Surgery (R.M.G.), Stony Brook University Medical Center, Stony Brook, New York; Department of Biomedical Engineering, Stony Brook University, Stony Brook, New York (A.S.K., T.F.F.); Department of Physics and Astronomy, University of Pennsylvania, Philadelphia, Pennsylvania (R.C.M., S.S.S., A.G.Y.); and Institute of Physics, University of Campinas, Campinas, São Paulo, Brazil (R.C.M.).

<zdoi;10.1097/ALN.0000000000000883>

of protracted ischemia upon nerve transmission,[14] and studies have demonstrated that the delay in nerve transmission variation from the onset of ischemia may exceed 20 min.[15] Furthermore, because evoked potential changes can also be influenced by hypothermia, limb ischemia, and anesthetic management,[16] the management decisions in response to these alerts are difficult. A device that could be used in a complimentary manner with evoked potentials could eliminate these problems.

We have developed a near-infrared optical device that can accurately monitor and immediately detect the occurrence of spinal cord ischemia.[17] The device is based on the principles of diffuse correlation spectroscopy (DCS) and diffuse optical spectroscopy (DOS), which have previously been used successfully in research to measure cerebral hemodynamics, in cancer diagnostics, and in muscle perfusion studies.[18,19] The technique uses near-infrared light to probe deep tissues (up to a few centimeters), has a high temporal resolution (approximately 2 to 3 s), is noninvasive, and is portable.[20] We previously published a proof-of-concept article reporting the general ability of the DCS/DOS device in detecting spinal cord blood flow and oxygenation. In this article, we extend that work to examine the sensitivity, accuracy, and precision of the first-generation device, focusing upon its application to the detection of changes in spinal cord hemodynamics associated with aortic occlusion, as might be encountered during thoracic aortic surgery. We also examine the temporal resolution of the device in comparison with MEPs.

Materials and Methods

Experiments were conducted in accordance with the Institutional Animal Care and Use Committee (Stony Brook, New York) guidelines.

Animal Model

A total of 16 adult Dorset sheep, approximately 2 yr of age and weighing 60 to 70 kg, were used. The sheep and human spines are close in bony dimensions, such as spinal canal depth and width, especially in the thoracic and lumbar spines.[21]

Due to the expense of our experiments, and the "proof-of-concept" phase at which it currently lies, we have conducted multiple experiments in many of our sheep when scientifically appropriate. Table 1 represents the interventions that were performed in each sheep.

Surgical and Anesthesia Procedures

Animals were pretreated with glycopyrrolate (0.02 mg/kg, IM). Anesthesia was induced with ketamine 10 to 20 mg/kg IM, animals were intubated, and anesthesia was maintained with isoflurane (1.5 to 3.0%).

Femoral and carotid arterial and intravenous cannulae were placed after anesthetic induction for the measurement of mean arterial pressure (MAP) and microsphere sampling, respectively. MAPs were monitored through blood pressure transducers connected to a PowerLab device (ADInstruments Inc., USA). A left thoracotomy was performed through the T5 to T6 interspaces to allow for placement of a left atrial catheter for microsphere injections and to allow for exposure to the aorta for clamping. Aortic clamping was achieved *via* placement of a cross-clamp across the aorta after thoracotomy, or *via* inflation of an intraaortic balloon placed in the left femoral artery, and was advanced to a level immediately below the common cephalic trunk.

The fiber-optic probe was placed *via* laminotomy (N = 5) or *via* percutaneous (N = 11) approaches into the epidural space. Because the potential clinical placement of the probe would be after a laminectomy or laminotomy for spine surgery and percutaneously for aortic surgery, we tested the

Table 1. The Various Interventions Performed in Each Sheep

	Interventions				
Sheep	Hypertension	Hypotension	Hypoxia	Aortic Occlusion	Epidural Balloon
Animal 1	x	x			
Animal 2	x			x	
Animal 3	x	x		x	
Animal 4	x	x	x	x	
Animal 5	x	x	x	x	
Animal 6	x			x	
Animal 7	x				x
Animal 8	x		x	x	
Animal 9					x
Animal 10				x	
Animal 11	x	x			
Animal 12	x	x			
Animal 13	x	x		x	
Animal 14	x	x			
Animal 15	x	x			x
Animal 16	x	x			

x = intervention was performed.

capability of the device to accurately measure the spinal cord hemodynamics through both probe placement techniques.

A posterior laminotomy was created to allow for open placement of the fiber-optic probe. After adequate general anesthesia was established, the sheep was positioned prone. A midline incision was made, and a subperiosteal dissection was performed to expose the spinous processes, lamina, and medial facets. A Leksell rongeur was then used to remove the intraspinous ligaments as well as the spinous processes themselves. A thin-footed Kerrison was used to carefully remove the lamina creating a trough that was sequentially widened until the dura of the spinal cord was well seen. The probe was placed using loupe magnification and was advanced superiorly or inferiorly under intact laminae to lie within the epidural space.

Percutaneous placement of the probe was achieved *via* 17-gauge Tuohy needle introduced in an L2 to L4 lumbar interspace, with the epidural space identified by loss of resistance to air or saline. The probe was then advanced to the desired level under fluoroscopic guidance (see video, Supplemental Digital Content 1, http://links.lww.com/ALN/B218, which shows the percutaneous placement of the fiber-optic probe and its advancement to the desired vertebral level under fluoroscopic guidance). Ventilatory rate and volume, systemic oxyhemoglobin saturation (pulse oximetry), electrocardiogram, end-tidal carbon dioxide, and MAP were continuously monitored.

Diffuse Optical Methods

The optical instrumentation uses both DCS and DOS. DOS is the widely used diffuse optical technique applied in both pulse and cerebral oximetry.[19,22] The wavelength-dependent differential absorption of near-infrared light can be quantitatively related to the concentrations of tissue chromophores such as oxyhemoglobin and deoxyhemoglobin in the microvasculature.[23]

Diffuse correlation spectroscopy is a novel optical technique used to measure blood flow in deep tissues by quantifying the temporal intensity fluctuations of the detected light.[19,20] These fluctuations arise mainly from moving light scatterers in tissue (*e.g.*, erythrocytes). In practice, the fluctuations are quantified by the decay rate of the temporal intensity autocorrelation function of the detected light; specifically, the decay rate of DCS autocorrelation function depends on the "average" flux of erythrocytes in the vasculature. Changes in spinal cord blood flow were estimated from the experimental DCS data by fitting the measured intensity autocorrelation function $g_1(\tau)$ to the solution of the photon correlation diffusion equation in the semi-infinite geometry (fig. 1).[24] The Brownian motion model was used to approximate the mean-square particle displacement of the erythrocytes in tissue and thus to derive the spinal cord blood flow index (BFI). Relative changes in blood flow (ΔBF) were calculated using $\Delta BF = BFI(t)/BFI(t0) - 1$, where $t0$ represents the baseline period.

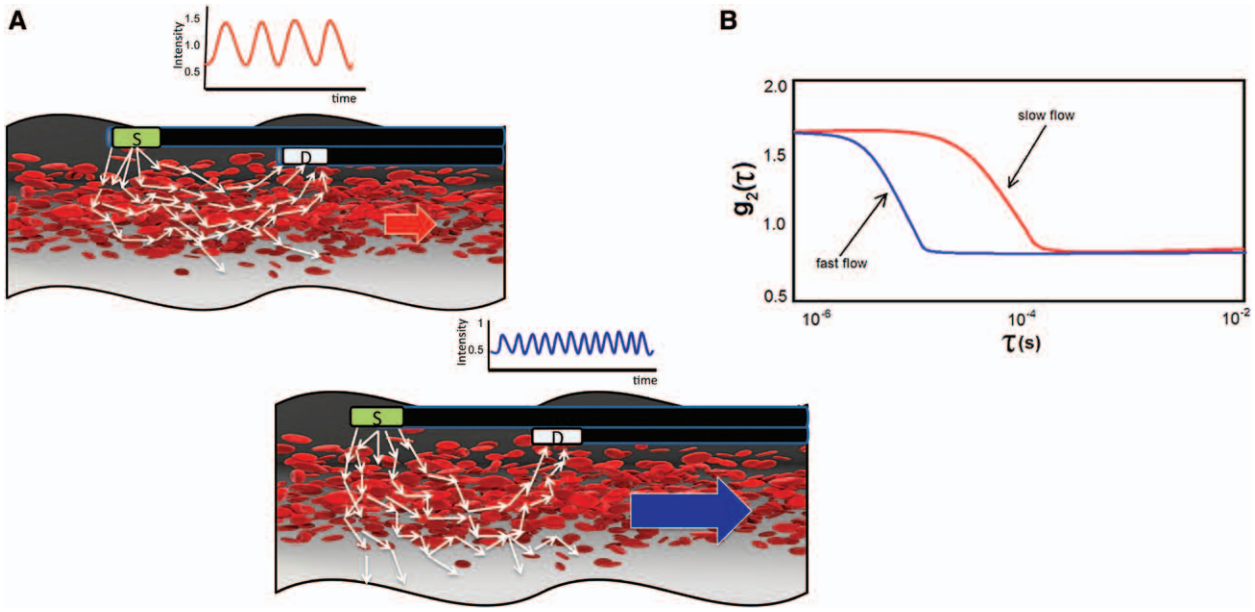

Fig. 1. Schematic of the diffuse correlation spectroscopy (DCS) measurement. (*A*) DCS measures the fluctuations of detected light intensity, which occur due to the motion of scatterers such as erythrocytes. The strength of the correlation in DCS signal between two time points depends on the movement of erythrocytes. Thus, higher blood flow (faster displacement of the erythrocytes, indicated by the *blue arrow*) leads to greater fluctuations in signal intensity and lower correlation of the DCS signal with itself, resulting in the faster decay of autocorrelation of the intensity detected at the output fibers. Lower displacement of erythrocytes (indicated by the *red arrow*) leads to a slower decay of the intensity autocorrelation function. (*B*) The fluctuations in light intensity detected by the avalanche photodiode detectors are fed to an autocorrelator that computes the normalized temporal intensity autocorrelation function $g_2(\tau)$ from photon arrival times. τ(s) represents the autocorrelation function time delay. D = detector fiber; S = source fiber.

Diffuse Optical Device

The device is composed of the fiber-optic probe and the monitor.

The Probe. For tissue monitors working in the reflection geometry, it has been empirically known that the mean optical penetration depth into tissue is roughly one half to one third of the source-detector (S-D) separation on the tissue surface.[25] Thus, the S-D separation plays an important role in determining the depth of tissue penetrated by the laser light, with greater S-D separation leading to greater optical penetration. For our experiments, we used a fiber-optic probe that has the look and feel of an epidural catheter. This probe was configured with a single source at its tip and detectors deployed at 1 and 2 cm behind the source, with corresponding penetration depths of approximately 0.4 to 1 cm (fig. 2). This thin, highly flexible probe can be placed either percutaneously through a 17-gauge Tuohy needle or through an open placement approach after a laminotomy.

The Monitor. The monitor, which collects data on blood flow (DCS) and oxygenation (DOS), is composed of two modules as described previously.[17] In brief, the DCS module uses a long-coherent, continuous-wave 785-nm laser (CrystaLaser Inc., USA) as a light source. The DOS module uses one source fiber switched between three amplitude modulated (70 MHz) laser diodes in the near infrared range (686, 785, and 830 nm). The DCS and DOS modules are integrated through a data acquisition board (National Instruments, USA).

Data Acquisition and Analysis

Diffuse correlation spectroscopy/DOS data were collected using LabView software code (National Instruments). Femoral and carotid MAPs were continuously recorded using a PowerLab device using LabChart software (ADInstruments) and a separate computer. The arterial monitoring and DCS/DOS data were correlated and analyzed offline using homemade MATLAB scripts (MathWorks, USA).

Sensitivity

In this study, we define sensitivity as the ability to detect acute changes in spinal cord blood flow and oxygenation associated with pharmacologic, physiologic, and proximal aortic occlusion.

We first characterized the sensitivity of the DCS/DOS device to detect changes in spinal cord blood flow and oxygenation associated with (1) acute hypertension induced *via* boluses of phenylephrine (400 μg) in 14 sheep, (2) acute hypotension induced *via* boluses of nitroprusside (400 μg) in

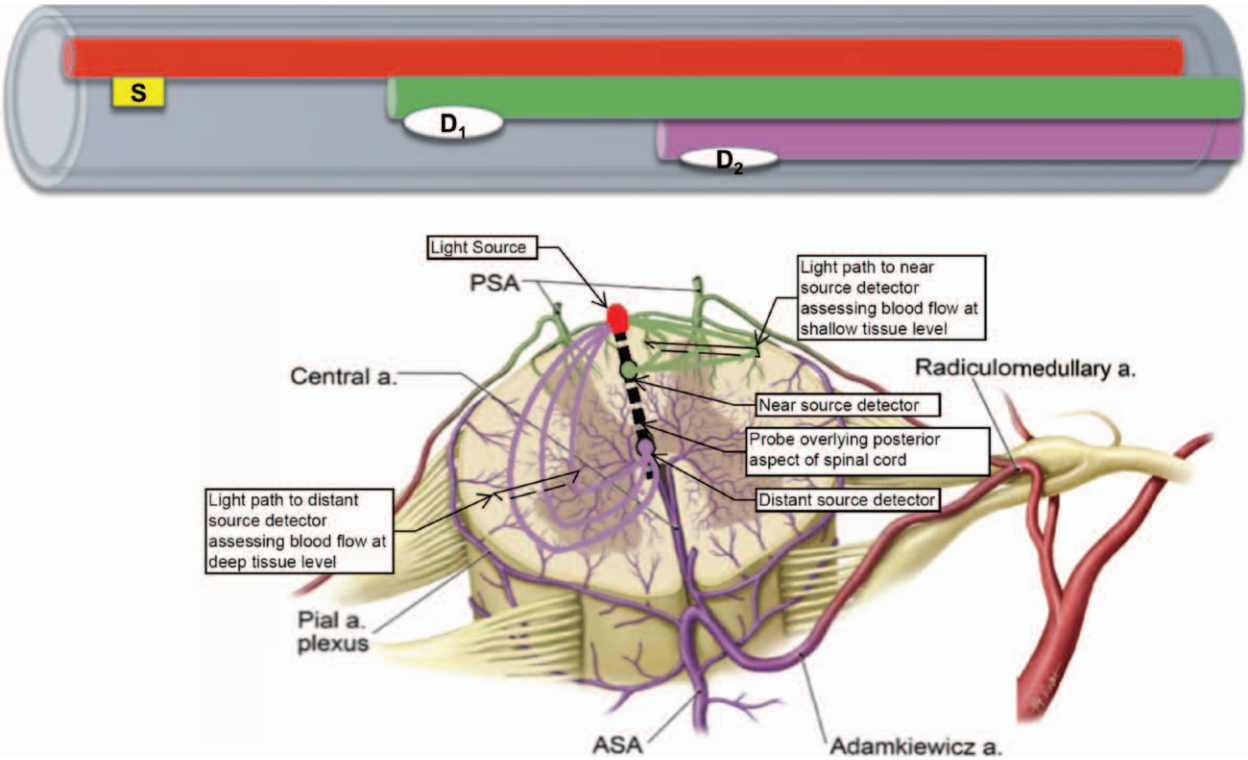

Fig. 2. The fiber-optic probe consists of one source (S) and two detectors at a separation of 1.0 cm (D1) and 2.0 cm (D2) from the source. The probe is placed overlying the posterior aspect of the spinal cord and can interrogate tissue depth of ≈ 0.4 to 1.0 cm. The detector closer to the source (D1, represented in *green*) interrogates more shallow tissues (bias toward posterior cord), whereas the farther detector (D2, represented in *purple*) measures blood flow in deeper tissues (bias toward anterior cord). ASA = anterior spinal artery; PSA = posterior spinal artery. Illustration showing vascularization of the lumbar spinal cord is modified and used with permission from Dr. Nicholas Theodore, M.D., Barrow Neurological Institute. Adaptations are themselves works protected by copyright. So in order to publish this adaptation, authorization must be obtained both from the owner of the copyright in the original work and from the owner of copyright in the translation or adaptation.

10 sheep, and (3) systemic hypoxia and hypercarbia, created *via* respiratory arrest until the systemic hemoglobin saturation reached ≈ 80% as measured by pulse oximeter in 3 sheep.

Next, the sensitivity of the DCS/DOS device in detecting changes in spinal cord blood flow and oxygenation associated with aortic occlusion was characterized. In eight sheep, spinal cord ischemia was elicited through occlusion of the aorta either by inflation of an intraaortic balloon (Cook Medical, USA) or by clamping the aorta after thoracotomy. Aortic occlusion was confirmed fluoroscopically *via* direct visual inspection through the open chest and *via* loss of femoral arterial pressure; aortic occlusion was maintained for 5 min.

Accuracy

The accuracy of the device was tested *via* comparison of DCS with microsphere spinal cord blood flow measurements. Nonradioactive stable isotope-labeled microspheres of 15-μm diameter were injected into the left atrium (10 ml, 2×10^6 microspheres per milliliter; STERIspheres, USA). Reference blood samples were withdrawn from the distal aorta *via* the femoral artery catheter at a rate of 600 ml/h over 3 min using a syringe pump (Harvard Apparatus, USA). Multiple measurements (n = 20) during interventions (nitroprusside: 400 μg bolus, phenylephrine: 400 μg bolus, aortic clamping) were performed through the use of multicolor microspheres in seven sheep. After euthanasia, the spinal cord was resected, labeled, and weighed. Spinal cord tissue blocks and blood samples were then prepared for subsequent analysis of microsphere concentrations and blood flow. We compared the percent change in blood flow from baseline detected by microspheres, with the percent change in BFI measured with DCS from baseline.

Spatial Accuracy

To rule out the possibility that the probe is measuring flow in tissue other than that of the spinal cord, we introduced a Fogarty balloon into the epidural space adjacent to the probe detectors in three sheep. The balloon was then inflated to compress the cord directly adjacent to the probe while flow was recorded. In addition, we placed the probe into the lumbar paraspinous muscles of the sheep and measured flow during aortic cross-clamping at the T4 and T8 levels.

Precision

The precision of the DCS flow measurement was assessed *via* analysis of the spinal cord blood flow measured at steady state over 4 h in four sheep. The DCS monitor measures one datapoint every 8 s. Here, we compared the repeatability of measurements taken every 10 min. Within-sheep coefficient of variation and repeatability were calculated as described previously using a root-mean-square approach.[26] In brief, we calculated the square of the coefficient of variation for each sheep separately, found its mean, and took the square root of this mean. We also report the estimated repeatability coefficient, calculated as $1.96 \times \sqrt{2} \times$ within-sheep SD. The repeatability coefficient could be interpreted as the upper limit of the absolute difference between two measurements on a subject to differ with 95% probability when the differences are approximately normally distributed.

Axial Resolution

In this study, we tested, in a single sheep, the hypothesis that spinal cord blood flow and oxygenation diminishes with increasing distance from the site of proximal aortic occlusion and from the sites of collateral blood flow originating from sources above the level of the occlusion. We thus attempted to demonstrate that the device could axially resolve differences in changes in blood flow and oxygenation during ischemia due to differences in vascular anatomy. Aortic occlusion was again achieved *via* inflation of an intraaortic balloon just below the common cephalic trunk and was maintained for 5 min. During sequential aortic occlusions, spinal cord blood flow and oxygenation were recorded with the probe placed at the vertebral levels T4, T7, T11, and L2. Before probe repositioning and repeated measurements, aortic occlusion was released and MAP allowed to recover to baseline. Corresponding microsphere measurements of spinal cord blood flow at baseline and after aortic occlusion at each level were conducted as described (see Accuracy under the section Materials and Methods).

Comparison with MEP Monitoring

Motor-evoked potential monitoring required transcranial stimulation of the motor cortex by electrical stimuli involving three to seven pulses of 100 to 400 V that produced a response that traveled down the corticospinal tracts and that generated a measurable muscle response, the compound muscle action potential. The disposable subdermal needle electrodes were placed according to the international 10 to 20 system.[27] The motor stimulus electrodes were placed a few centimeters behind the Cz plane at C3' to C4'. The motor recording electrodes were placed in the semimembranosus or gastrocnemius muscles in the lower extremities and in the flexor carpi ulnaris for upper limb MEP recording. The anesthetic agent was ketamine 200 mg/h *via* infusion during these experiments.

The most commonly used criteria for alerting to a clinically relevant event during MEP monitoring is either a 100 or 80% loss of signal.[28] Therefore, the time for DCS to detect a 50% drop in blood flow from baseline was compared with the time for MEP signals to drop by 80% from baseline upon performing an aortic clamping in three sheep. The time for the DCS and evoked potential signal to recover back to baseline after unclamping was also compared.

Statistical Analysis

The changes due to the various pharmacological and mechanical interventions were calculated from the highest or lowest blood flow and oxygenation value in the time course during the intervention period. For each intervention, mean change and SD were calculated by averaging over all trials and animals. Nonparametric Wilcoxon signed-rank tests were used to assess whether there

was a statistically significant difference between the observed blood flow/oxygenation changes from those at baseline.

Spinal cord blood flow measured by the DCS and microsphere techniques was compared by correlating the simultaneous point measurements across all animals and trials. The degree of correlation was measured by the Pearson correlation coefficient. The ratios of DCS changes to microsphere changes from baseline were obtained from the slope of the curve. All data analyses were performed with MATLAB (MathWorks Inc.), and statistical analysis was performed with JMP software (SAS Institute, USA). A paired *t* test was used to determine whether the correlation between the blood flow changes detected by microspheres and DCS was statistically significant. Nonparametric Wilcoxon signed-rank test was used to determine whether the time taken by DCS and evoked potentials to drop/recover upon aortic clamping/unclamping was statistically different. Data were analyzed using JMP statistical software (SAS Institute).

Results

Table 2 summarizes the blood flow and oxygenation changes observed with each type of intervention.

Sensitivity

One hundred percent changes in blood flow and oxygenation were detected upon administering pharmacological interventions designed to elicit acute hypertension (65 of 65 trials) and hypotension (48 of 48 trials) or upon creating hypoxia/hypercarbia (4 of 4 trials) and aortic occlusion (32 of 32 trials).

Acute hypertension, elicited *via* 400-μg boluses of phenylephrine or vasopressin, resulted in an expected transient increase in spinal cord blood flow (+48 ± 21%, n = 65 interventions) and oxyhemoglobin concentration (+4 ± 2%, n = 13 interventions). A representative example of increase in blood flow in one trial is shown in figure 3A. Hypotension, elicited *via* bolus of nitroprusside (400 μg), resulted in the expected decrease in blood flow (–48 ± 11%, n = 48 interventions) and oxyhemoglobin (–6 ± 1%, n = 9 interventions). A brief hyperemic response followed in all cases (fig. 3B shows an example). Spinal cord blood flow and oxygenation changes measured by DCS and DOS closely paralleled the changes in femoral and carotid MAPs. Hypoxia and hypercarbia, elicited *via* respiratory arrest, resulted in an increase in blood flow (+84 ± 22%, n = 4 interventions), as shown in a representative example in figure 3C, and decrease in oxygenation (–9 ± 6%, n = 4 interventions).

During aortic occlusion, confirmed by hypotension recorded in the femoral artery and hypertension recorded in the carotid artery, spinal cord blood flow (fig. 4A) and oxygenation (fig. 4B) decreased immediately in response to occlusion by –65 ± 32% (n = 32) and –17 ± 13% (n = 11), respectively. Aortic unclamping resulted in a hyperemic flow and oxygenation response. Wilcoxon signed-rank test showed statistically significant difference in BFI from baseline for the 32 trials ($P < 0.0001$). Aortic occlusion yielded similar results when the probe was placed *via* laminectomy (N = 6) or percutaneous (N = 4) approaches.

Accuracy

Diffuse correlation spectroscopy and microspheres were used to measure blood flow changes immediately after performing the following interventions: 400-μg phenylephrine bolus (n = 6), 400-μg nitroprusside bolus (n = 4), and aortic occlusion (n = 10). Peak or nadir changes in blood flow during continuous monitoring of DCS correlated reasonably well with the changes measured with microspheres after a single injection during the intervention ($R^2 = 0.49$, $P < 0.01$; fig. 5).

Spatial Accuracy

Upon epidural balloon inflation, there was an immediate drop in spinal cord blood flow (–75 ± 14%, n = 3) and oxygenation (–10 ± 6%, n = 3), which recovered as soon as the balloon was released (an example is shown in fig. 6). With the probe placed in the paraspinous muscle, 500-μg phenylephrine boluses (n = 5) and aortic clamping (n = 2) resulted in no significant changes in flow detected by the optical device. This further confirms that the optical device measures only spinal cord blood flow and not blood flow from surrounding muscle or vessels is contributing to the measurements.

Precision

The DCS BFI values were averaged every 10 min during 4 uninterrupted hours of monitoring, in four sheep, to test the repeatability of the device. The mean ± SD, between-sheep and within-sheep coefficients of variation, and group repeatability coefficient are reported in table 3.

Table 2. Summary of the Blood Flow and Oxygenation Changes Observed with Each Type of Intervention Performed

		Blood Flow		Oxygenation	
Intervention	No. of Sheep	Mean Changes (%)	No. of Trials	Mean Changes (%)	No. of Trials
Hypertension—400 μg phenylephrine	14	48 ± 21	65	4 ± 2	13
Hypotension—400 μg nitroprusside	10	–48 ± 11	48	–6 ± 1	9
Hypoxia	3	84 ± 22	4	–9 ± 6	4
Aortic occlusion	8	–65 ± 32	32	–17 ± 13	11
Epidural balloon	3	–75 ± 14	10	–10 ± 6	3

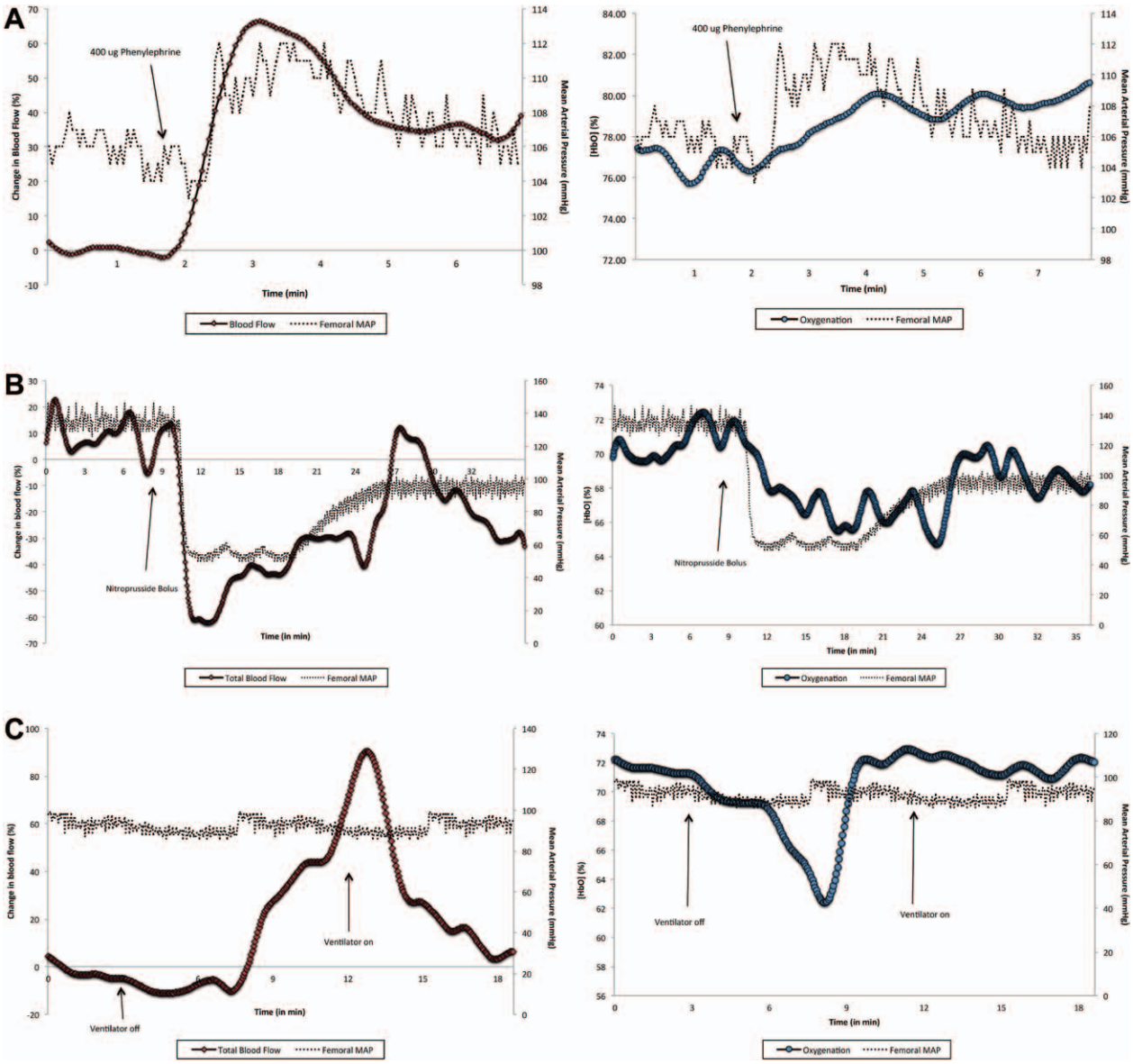

Fig. 3. (*A*) Hypertension from vasopressor boluses (phenylephrine and vasopressin) transiently increased the blood flow. (*B*) Hypotension from vasodilator boluses (nitroprusside) caused a transient decrease in blood flow. (*C*) Withholding ventilation causing hypoxia and hypercarbia resulted in increased blood flow. In all three cases, the x-axis represents time in minutes and the y-axis represents the percentage of change in the blood flow index. MAP = mean arterial pressure.

Axial Resolution

The device detected a greater diminution in spinal cord blood flow during aortic occlusion with increasing distance from the proximal aortic occlusion site, as we hypothesized. Spinal cord blood flow decreased by 62% (T4 level), 65% (T7 level), 89% (T11 level), and 90% (L2 level), whereas oxygenation decreased by 18% (T4 level), 23% (T7 level), 40% (T11 level), and 40% (L2 level), as shown in figure 7.

Comparison with MEP Monitoring

Upon proximal aortic clamping in three sheep, it took an average of 2 min for the blood flow detected by DCS to drop by 50% from baseline. The mean time taken for an 80% drop in amplitude of evoked potential signal was 16 min, an example of which is shown in figure 8. After the clamp was released, the DCS signal returned back to baseline in 1 min, whereas it took approximately 18 min for evoked potentials to return back to baseline. Nonparametric Wilcoxon signed-rank tests showed statistically significant difference between the time taken for DCS and evoked potential signals to drop upon clamping ($P = 0.03$) and recover upon unclamping ($P = 0.03$).

Discussion

The fiber-optic probe and monitoring device reliably detected spinal cord responses to pharmacologic and

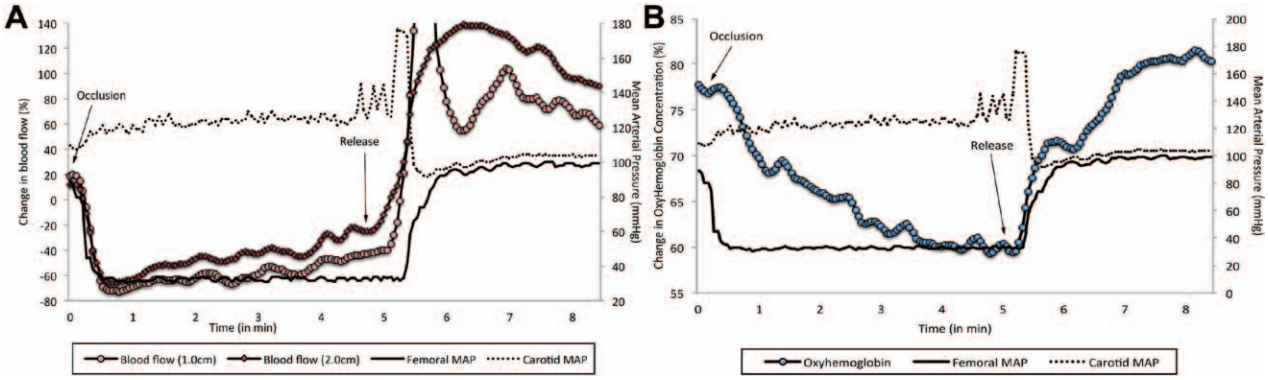

Fig. 4. Aortic occlusion resulted in a −65 ± 32% decrease in blood flow in 32 of 32 trials and a −17 ± 13% decrease in oxygenation in 11 of 11 trials. This figure represents one aortic occlusion trial, which resulted in (*A*) a blood flow decrease of ≈ 85% and (*B*) an oxygenation decrease of ≈ 39%, respectively. The x-axis represents time in minutes, and the y-axis represents the percentage of change in the blood flow detected by diffuse correlation spectroscopy (*A*) and diffuse optical spectroscopy (*B*). MAP = mean arterial pressure.

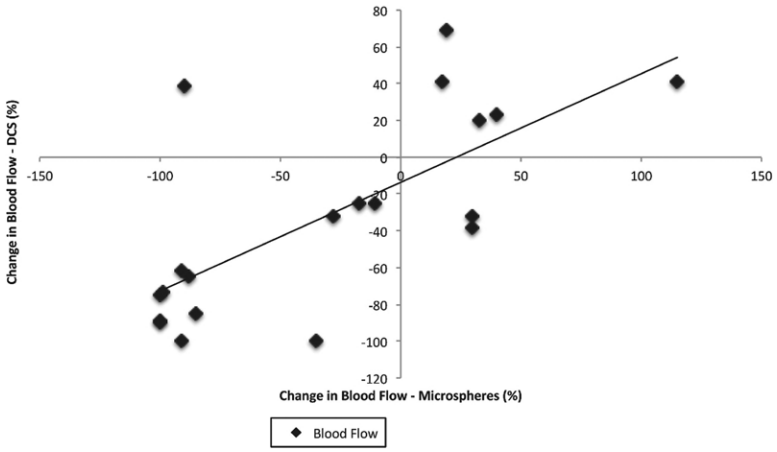

Fig. 5. Scatter plot representing the Pearson correlation between microsphere and diffuse correlation spectroscopy (DCS) measurements of blood flow changes (R^2 = 0.49, P < 0.01, n = 22). The x-axis represents the percent change in blood flow detected by microspheres, whereas the y-axis represents the percent change in blood flow detected by DCS.

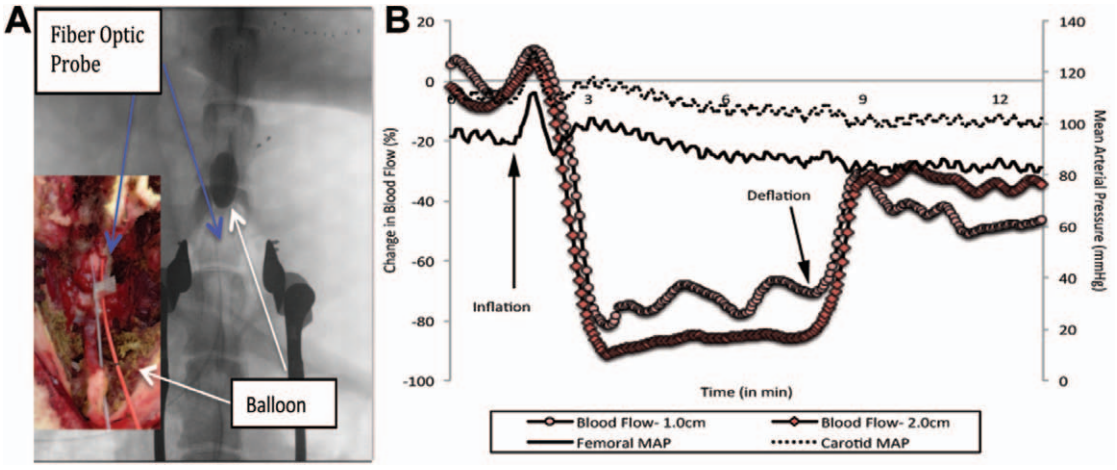

Fig. 6. A 6-Fr Fogarty balloon was inflated in the epidural space directly onto the spinal cord. (*A*) Radiographic image and photograph showing location of the probe and balloon on the spinal cord. (*B*) The probe, placed at the site of injury, immediately detected a drop in blood flow, which recovered soon after the balloon was deflated. The x-axis represents time in minutes and the y-axis represents the percentage of change in the blood flow detected by diffuse correlation spectroscopy. MAP = mean arterial pressure.

Table 3. The Repeatability Coefficient Was Calculated with a 95% CI by Using a Root Mean Square Approach According to Bland–Altman

	10 Min			
Sheep	Mean ± SD*	Between-sheep Coefficient of Variation, %	Within-sheep Coefficient of Variation, %	Repeatability Coefficient, %
1	14.02 ± 1.17	24.60	9.69	26.80
2	8.66 ± 1.08			
3	13.23 ± 1.32			
4	9.09 ± 0.68			

Diffuse correlation spectroscopy was used to measure the blood flow index in four sheep at steady state (baseline) over 4 h. The repeatability coefficient of 26.8% indicates that the absolute difference between two measurements on a sheep would have a 95% probability to differ by no more than 26.8%.

* Means and SDs of each sheep's blood flow index values measured by diffuse correlation spectroscopy in corresponding time scales.

physiologic interventions; the detected responses were in line with published data.[29] Boluses of hypertensive agents created brief periods of hypertension, which were accompanied by brief increases in spinal cord blood flow and oxygenation. Boluses of nitroprusside produced brief periods of hypotension and corresponding decrement in spinal cord blood flow and oxygenation. Breath holding, resulting in hypoxia and hypercarbia, induced a gradual increase in flow and decrement in oxygenation. Clamping the aorta resulted in a rapid decrement in blood flow and a slower decrement in tissue oxygenation. Unclamping the aorta resulted in a hyperemic overshoot from baseline. The responses to all interventions were robust, immediate, and reproducible. In all cases, changes in flow are more immediately responsive than changes in oxygenation. With hypotension, changes in blood pressure and blood flow always preceded slower changes in oxygenation. With hypertension, oxyhemoglobin saturation, already near maximal, should not be expected to but marginally increase. With respiratory arrest, hypercarbia precedes the occurrence of hypoxia, eliciting a gradual increase in flow and much slower decrease in oxygenation.

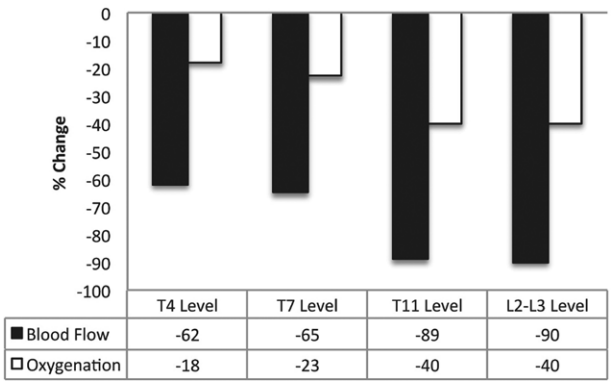

Fig. 7. This figure depicts the percent change in blood flow (*black bars*) and oxygenation (*white bars*) detected at the T4, T7, T11, and L2 to L3 vertebral levels, respectively. Clamping the proximal descending thoracic aorta cuts off blood supply from intercostal arteries, making the spinal cord flow heavily dependent on flow from vertebral arteries above the occlusion site. One would then expect a greater decrease in blood flow and oxygenation the farther one moves away from the occlusion site and vertebral artery sources. Flow and oxygenation measurements made sequentially from T4 to L3 during proximal aortic occlusion documented this pattern.

The shorter S-D separations are biased to interrogating and measuring flow in the posterior circulation closest to the probe, whereas the longer separations would be biased toward interrogating and measuring flow in the more distant anterior circulation. In this study, we have averaged the flow and oxygenation measured by both detectors. Working out the ability of the probe to spatially resolve flow and oxygenation in the anterior and posterior circulations is a long-term goal of this research.

Although thoracic aortic clamping can be expected to result in diminished flow not only to the spinal cord, but also to the aorta and paraspinous muscles, epidural balloon inflation onto the spinal cord creates a localized decrease in blood flow only in the spinal cord, leaving flow in surrounding muscles and vessels intact. As inflation of the balloon over the probe resulted in a near-complete and instantaneous loss of blood flow, we can therefore conclude that the probe was not measuring flow in the aorta, paraspinous muscles, or other source. Furthermore, it has been established that while paraspinous muscles (and all muscle for that matter) have a rich vascular supply,[30] baseline muscle blood flow under rest conditions is almost too low to measure by any clinically applicable technique.[31] Thus, the lack of detection of significant blood flow changes by the optical device upon phenylephrine boluses and aortic clamping when the probe was positioned in the paraspinous muscle can be attributed to this extremely low blood flow and further documents that the paraspinous muscles are not the source of changes in blood flow detected by our device.

The accuracy of the blood flow changes measured by the optical probe was difficult to determine due to the fact that no true "accepted standard" exists for the measurement of spinal cord blood flow. The microsphere measurements and DCS measurements of spinal cord blood flow have some differences that make a direct comparison between the two methods difficult. DCS has high temporal resolution (milliseconds) and offers continuous measurements, but the units of the DCS BFI are not the same as absolute flow units. On the contrary, microsphere measurements require minutes to complete but offer quantitative measurements

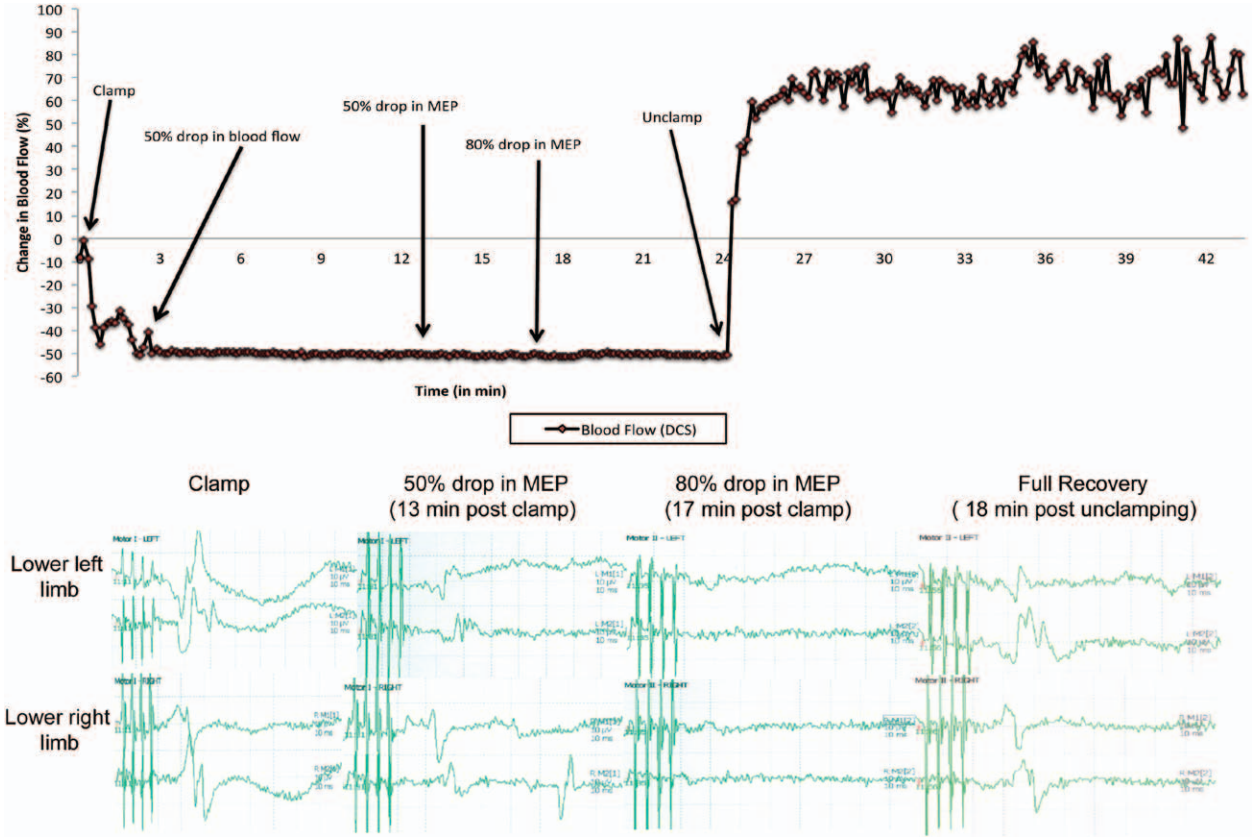

Fig. 8. In three sheep, the time taken by diffuse correlation spectroscopy (DCS) to detect a 50% decrease in blood flow from baseline was compared with the time taken by motor-evoked potential (MEP) monitoring to detect an 80% decrease in its signal upon aortic clamping. As shown in this representative example, DCS took 3 min to detect a 50% decrease in blood flow from baseline, whereas it took 17 min to detect an 80% loss of amplitude in MEP signal. Although DCS detected blood flow recovery immediately (1 min), it took the MEP signal 18 min to return back to baseline after the clamp was removed.

of flow (in absolute units). Thus, it is not possible to exactly match the DCS peak or nadir measurement with the microsphere measurement as observed in our data. Microsphere measurements in the spinal cord can be challenging for other reasons. The entire spinal cord, in a 50-kg sheep, weighs between 20 to 25 g. Spinal cord blood flow is reported to be in the range of 20 to 40 ml per 100 g/min. In a 50-kg sheep, with a 4-l/min cardiac output, the cord receives approximately 10 ml/min or 0.25% of the total cardiac output. The fraction of microspheres injected reaching the cord is then 0.25%, and the sampled volume of spinal cord analyzed is approximately 2 to 5 g. Thus, microsphere measurements are themselves challenged by a number of factors severely limiting their own accuracy. An alternative method for comparison might be laser Doppler flowmetry (LDF). LDF has high temporal resolution; however, unfortunately, its depth of penetration is limited to less than 0.5 mm. An LDF probe, placed upon the posterior cord, for example, would provide very little information about flow in the anterior spinal cord, the area of greatest interest. The DCS/DOS device offers not only high temporal resolution but can also interrogate the entire depth of the spinal cord. Thus, although there was a reasonably good correlation between the DCS and microsphere measurements, the differences in the techniques may explain the lack of an excellent correlation curve.

A point of reference with which to interpret our precision estimates made with DCS can be found *via* comparison with those made with the accepted standard for brain blood flow, positron emission tomography. Precision assessments are typically made under steady-state conditions, such as have been reported for positron emission tomography in brain.[32] Carroll *et al.*, in a group of 10 subjects, and comparing three measurements within 45 min in each subject, conducted on days 1 and 3 reported an intersubject reproducibility coefficient of ± 24% for gray matter and ± 34% for white matter in brain.

In humans, it is well documented that the proximal to midthoracic anterior spinal cord receives a significant contribution from the vertebral arteries.[33] More distal aspects of the thoracic and lumbar spinal cord are dependent on blood supply directly from the descending thoracic and abdominal aorta. Multiple reports establish the unpredictable and diffuse nature of the blood supply to the spinal cord.[34,35] This unpredictable blood supply demands a monitoring technique that is not discretely focused upon a single level. The second-generation probes that we have designed will allow

for the mapping and axial resolution of spinal cord blood flow and oxygenation, from superior to inferior spinal cord levels, across a distance of 20 to 50 cm. Such a probe could be positioned or centered on a considerably broad "region" considered at risk.

In addition to the high degree of sensitivity of the DCS/DOS device that we have reported, the immediacy of the response to aortic clamping deserves special note. Published reports suggest that current evoked potential monitoring technology produces a lag from the insult to alert, and this lag time can approach 20 min.[12] Our data in sheep confirm this. This difference in response to time between DCS and evoked potentials in alerting the surgeon or anesthesiologist to the decrement in blood flow may have important implications for a surgeon attempting to address the ischemia. The clinical impact of such a delay is compounded by the fact that evoked potentials are also associated with a profound delay in recovery of signal. On the contrary, DCS immediately identifies the restoration of flow. Therefore, DCS may have important advantages over evoked potentials in alerting the surgeon to the onset of ischemia as well as signaling when an attempt at restoration has been successful.

Because the optical device measures relative changes in blood flow, it is not likely to be affected by patient temperature, anesthetic agents, or decrement in blood flow to a lower limb, which commonly frustrate evoked potential monitoring. When used in conjunction with evoked potential monitoring, this device could allow for the ability to discriminate between cord and nerve root injury during spine surgery. Used in tandem, they could also better discriminate the contribution of anesthetics and peripheral ischemic issues, such as an ischemic leg during femoral cannulation for cardiopulmonary bypass, that frequently impair evoked potential signals unilaterally.

Probes when placed by open approaches might be used by a neurosurgeon or orthopedic spine surgeon or when placed *via* percutaneous approaches might be used when spine surgery was not planned, such as for aortic surgery, or in the neurocritical care environment to manage spine injury before surgery. The demonstrated ability to place the highly flexible DCS/DOS probe using a percutaneous approach that replicates the approach to the placement of epidural catheters may lower the barrier to acceptance of the device by anesthesiologists and critical care specialists.

Although the DCS/DOS device described herein may offer more immediate and reliable detection of spinal cord ischemia than conventional methods such as evoked potentials, it is reasonable to question whether interventions designed to alleviate detected ischemia may actually have the capacity to reverse the ischemic insult, and whether improved monitoring might actually impact outcome. It would be ideal to know before committing to aortic grafting just what impact the graft might have upon spinal cord blood flow. The device described herein could be placed before surgery or at least before commitment to grafting. A trial aortic occlusion or stent deployment might be performed, during which spinal cord blood flow is monitored. An "unsafe" drop in spinal cord blood flow might allow the surgeon to reevaluate the neurologic risk associated with the proposed procedure. Finally, because the probe can remain in place after surgery, it offers the opportunity for postoperative monitoring and management of patients in the intensive care unit, providing feedback for the impact of cerebrospinal fluid drainage or hemodynamic support upon spinal cord blood flow and oxygenation.

Acknowledgments

The authors thank the Biostatistical Consulting Core at Stony Brook University (Stony Brook, New York) for consulting with them on the statistical analysis. The authors also thank the veterinary technicians at the Division of Laboratory Animal Resources (DLAR) at Stony Brook University and Cecille Just, an electroencephalography (EEG) specialist, from the EEG Department at Stony Brook Hospital (Stony Brook, New York), for their assistance with their sheep experiments.

This work has been supported by the Craig H. Neilsen Foundation (Encino, California); Stony Brook University Fusion Award (Stony Brook, New York); Stony Brook University's Department of Anesthesiology; Office of the Vice President for Research; School of Medicine and University Hospital (Stony Brook, New York; to Drs. Floyd and Kogler); National Institutes of Health (Bethesda, Maryland; grant nos. R01-NS060653 and P41-EB015893 to Dr. Yodh); and the São Paulo Research Foundation through grant no. 2012/02500-8 (São Paulo, Brazil; to Dr. Galler).

Competing Interests

Dr. Floyd has registered a company, NFOSYS, Inc. (Media, Pennsylvania). It is anticipated that this company will attempt to commercialize the device described herein over the next 3 to 5 yr. The other authors declare no competing interests.

Correspondence

Address correspondence to Dr. Floyd: Stony Brook University Hospital, Department of Anesthesiology, HSC-Level 4, # 073-C, Stony Brook, New York. thomas.floyd@stonybrookmedicine.edu. Information on purchasing reprints may be found at www.anesthesiology.org or on the masthead page at the beginning of this issue. Anesthesiology's articles are made freely accessible to all readers, for personal use only, 6 months from the cover date of the issue.

References

1. Becker DA, McGarvey ML, Rojvirat C, Bavaria JE, Messé SR: Predictors of outcome in patients with spinal cord ischemia after open aortic repair. Neurocrit Care 2013; 18:70–4
2. Conrad MF, Crawford RS, Davison JK, Cambria RP: Thoracoabdominal aneurysm repair: A 20-year perspective. Ann Thorac Surg 2007; 83:S856–61; discussion S890–2
3. Messé SR, Bavaria JE, Mullen M, Cheung AT, Davis R, Augoustides JG, Gutsche J, Woo EY, Szeto WY, Pochettino A, Woo YJ, Kasner SE, McGarvey M: Neurologic outcomes from high risk descending thoracic and thoracoabdominal aortic operations in the era of endovascular repair. Neurocrit Care 2008; 9:344–51

4. Hughes GC, Andersen ND, Hanna JM, McCann RL: Thoracoabdominal aortic aneurysm: Hybrid repair outcomes. Ann Cardiothorac Surg 2012; 1:311–9
5. Wong DR, Parenti JL, Green SY, Chowdhary V, Liao JM, Zarda S, Huh J, LeMaire SA, Coselli JS: Open repair of thoracoabdominal aortic aneurysm in the modern surgical era: Contemporary outcomes in 509 patients. J Am Coll Surg 2011; 212:569–79; discussion 579–81
6. Etz CD, Halstead JC, Spielvogel D, Shahani R, Lazala R, Homann TM, Weisz DJ, Plestis K, Griepp RB: Thoracic and thoracoabdominal aneurysm repair: Is reimplantation of spinal cord arteries a waste of time? Ann Thorac Surg 2006; 82:1670–7
7. Khan SN, Stansby G: Cerebrospinal fluid drainage for thoracic and thoracoabdominal aortic aneurysm surgery. Cochrane Database Syst Rev 2012; 10:CD003635
8. Patil CG, Patil TS, Lad SP, Boakye M: Complications and outcomes after spinal cord tumor resection in the United States from 1993 to 2002. Spinal Cord 2008; 46:375–9
9. Reames DL, Smith JS, Fu KM, Polly DW Jr, Ames CP, Berven SH, Perra JH, Glassman SD, McCarthy RE, Knapp RD Jr, Heary R, Shaffrey CI; Scoliosis Research Society Morbidity and Mortality Committee: Complications in the surgical treatment of 19,360 cases of pediatric scoliosis: A review of the Scoliosis Research Society Morbidity and Mortality database. Spine (Phila Pa 1976) 2011; 36:1484–91
10. Keyhani K, Miller CC III, Estrera AL, Wegryn T, Sheinbaum R, Safi HJ: Analysis of motor and somatosensory evoked potentials during thoracic and thoracoabdominal aortic aneurysm repair. J Vasc Surg 2009; 49:36–41
11. Nuwer MR, Dawson EG, Carlson LG, Kanim LE, Sherman JE: Somatosensory evoked potential spinal cord monitoring reduces neurologic deficits after scoliosis surgery: Results of a large multicenter survey. Electroencephalogr Clin Neurophysiol 1995; 96:6–11
12. Nuwer MR, Emerson RG, Galloway G, Legatt AD, Lopez J, Minahan R, Yamada T, Goodin DS, Armon C, Chaudhry V, Gronseth GS, Harden CL; American Association of Neuromuscular and Electrodiagnostic Medicine: Evidence-based guideline update: Intraoperative spinal monitoring with somatosensory and transcranial electrical motor evoked potentials. J Clin Neurophysiol 2012; 29:101–8
13. Hong JY, Suh SW, Modi HN, Hur CY, Song HR, Park JH: False negative and positive motor evoked potentials in one patient: Is single motor evoked potential monitoring reliable method? A case report and literature review. Spine (Phila Pa 1976) 2010; 35:E912–6
14. Seyal M, Mull B: Mechanisms of signal change during intraoperative somatosensory evoked potential monitoring of the spinal cord. J Clin Neurophysiol 2002; 19: 409–15
15. Kakinohana M, Abe M, Miyata Y, Oshiro M, Saikawa S, Arakaki K, Kuniyoshi Y, Sugahara K: Delayed response of transcranial myogenic motor-evoked potential monitoring to spinal cord ischemia during repair surgery for descending thoracic aortic aneurysm. J Anesth 2008; 22:304–7
16. Hofmeijer J, Franssen H, van Schelven LJ, van Putten MJ: Why are sensory axons more vulnerable for ischemia than motor axons? PLoS One 2013; 8:e67113
17. Mesquita RC, D'Souza A, Bilfinger TV, Galler RM, Emanuel A, Schenkel SS, Yodh AG, Floyd TF: Optical monitoring and detection of spinal cord ischemia. PLoS One 2013; 8:e83370
18. Yodh AG: Diffuse optics for monitoring brain hemodynamics. Conf Proc IEEE Eng Med Biol Soc 2009; 2009:1991–3
19. Lin Y, He L, Shang Y, Yu G: Noncontact diffuse correlation spectroscopy for noninvasive deep tissue blood flow measurement. J Biomed Opt 2012; 17:010502
20. Mesquita RC, Skuli N, Kim MN, Liang J, Schenkel S, Majmundar AJ, Simon MC, Yodh AG: Hemodynamic and metabolic diffuse optical monitoring in a mouse model of hindlimb ischemia. Biomed Opt Express 2010; 1:1173–87
21. Sheng SR, Wang XY, Xu HZ, Zhu GQ, Zhou YF: Anatomy of large animal spines and its comparison to the human spine: A systematic review. Eur Spine J 2010; 19:46–56
22. Boas DA, Campbell LE, Yodh AG: Scattering and imaging with diffusing temporal field correlations. Phys Rev Lett 1995; 75:1855–8
23. Yu G, Floyd TF, Durduran T, Zhou C, Wang J, Detre JA, Yodh AG: Validation of diffuse correlation spectroscopy for muscle blood flow with concurrent arterial spin labeled perfusion MRI. Opt Express 2007; 15:1064–75
24. Mesquita RC, Durduran T, Yu G, Buckley EM, Kim MN, Zhou C, Choe R, Sunar U, Yodh AG: Direct measurement of tissue blood flow and metabolism with diffuse optics. Philos Trans A Math Phys Eng Sci 2011; 369:4390–406
25. Patterson MS, Andersson-Engels S, Wilson BC, Osei EK: Absorption spectroscopy in tissue-simulating materials: A theoretical and experimental study of photon paths. Appl Opt 1995; 34:22–30
26. Bland JM, Altman DG: Agreement between methods of measurement with multiple observations per individual. J Biopharm Stat 2007; 17:571–82
27. Macdonald DB: Intraoperative motor evoked potential monitoring: Overview and update. J Clin Monit Comput 2006; 20:347–77
28. Langeloo DD, Lelivelt A, Louis Journée H, Slappendel R, de Kleuver M: Transcranial electrical motor-evoked potential monitoring during surgery for spinal deformity: A study of 145 patients. Spine (Phila Pa 1976) 2003; 28:1043–50
29. Izumi S, Okada K, Hasegawa T, Omura A, Munakata H, Matsumori M, Okita Y: Augmentation of systemic blood pressure during spinal cord ischemia to prevent postoperative paraplegia after aortic surgery in a rabbit model. J Thorac Cardiovasc Surg 2010; 139:1261–8
30. Griepp EB, Di Luozzo G, Schray D, Stefanovic A, Geisbüsch S, Griepp RB: The anatomy of the spinal cord collateral circulation. Ann Cardiothorac Surg 2012; 1:350–7
31. Elia M, Kurpad A: What is the blood flow to resting human muscle? Clin Sci (Lond) 1993; 84:559–63
32. Carroll TJ, Teneggi V, Jobin M, Squassante L, Treyer V, Hany TF, Burger C, Wang L, Bye A, Von Schulthess GK, Buck A: Absolute quantification of cerebral blood flow with magnetic resonance, reproducibility of the method, and comparison with H2(15)O positron emission tomography. J Cereb Blood Flow Metab 2002; 22:1149–56
33. Martirosyan NL, Feuerstein JS, Theodore N, Cavalcanti DD, Spetzler RF, Preul MC: Blood supply and vascular reactivity of the spinal cord under normal and pathological conditions. J Neurosurg Spine 2011; 15:238–51
34. Gillilan LA: The arterial blood supply of the human spinal cord. J Comp Neurol 1958; 110:75–103
35. Jacobs MJ, de Mol BA, Elenbaas T, Mess WH, Kalkman CJ, Schurink GW, Mochtar B: Spinal cord blood supply in patients with thoracoabdominal aortic aneurysms. J Vasc Surg 2002; 35:30–7